LIGHTNING DATA AND STUDY OF THUNDERSTORM NOWCASTING *

Qie Xiushu (郄秀书), *Yan Muhong* (言穆弘), *Guo Changming* (郭昌明) and *Zhang Guangshu* (张广庶)

Lanzhou Institute of Plateau Atmospheric Physics, Academia Sinica, Lanzhou 730000

Received March 27, 1991; revised June 26, 1992

ABSTRACT

From June 30 to September 14, 1989, about 2000 cloud–to–ground lightning location data have been collected by a three–direction–finder network in Beijing. These data have been used to study the spatial distribution of lightning including thunderstorm day, thunder density and thunderstorm hour. As a result of the terrain elevation, a clearly identifiable influence from the underlying topography was found. The lightning activity was mainly concentrated on the sunny side of the mountain, i.e., the east slope of Taihang Mountain, then eastward along the south side of Yanshan Mountain.

The comparison analysis of lightning data and radar echoes from several mesoscale convective systems in 1989 and 1990 suggests that lightning data can be used to determine the convective activity, its development probability and intensity. It can also be used to identify the different stages of a storm. The grid lightning data may be used in regional forecasting of storm. Case analysis shows that it is possible to forecast the position of active echo 30 minutes to an hour after lightning occurrence by using grid lightning data.

Key words: mesoscale convective system, ground lightning, regional forecasting

I. INTRODUCTION

The improved lightning location system (LLS) can provide information on occurring time, location, intensity and strike number of lightning in quasi–real time within a large region with small error and high detection efficiency. In the United States, LLS has been used in early detection of lightning–caused forest fires, the protection and dispatch of electricity system, the guarantee of aviation and space flight, the monitoring of thunderstorm and the warning of impending lightning (Krider et al., 1980; Fisher and Krider, 1982; Johnson et al., 1982). Since cloud–to–ground lightning data detected by LLS are the indicator of convective activity, and it is the only means to provide the two–dimensional lightning distribution in real time, National Weather Service has used LLS combined with lightning mapping systems to infer the developing and motion of convective storms (Rasch and Mathewson, 1983). The four users of lightning data of NSSFC, i.e., SELS, MD, convective SIGMET, FA, have got a preliminary result in forecasting the convective activity by using lightning data since 1988 when lightning monitoring system was installed (Lewis, 1989). They found that the real–time lightning data can be used in the operational forecastings of convective activity, including the presence, emergence, movement, dissipating, shape, range, intensity and reproduction of the storm.

* This work is supported by National Natural Science Foundation of China.

Three direction–finders (DFs) and a position analyser (PA) produced by LLP Incorporation together with a successive processing system developed by ourself constitute the LLS which has been operated in State Meteorological Administration, Beijing, for several years as a special observational tool in Severe Storm Laboratory. The observation suggests that LLS maybe have its superiority in nowcasting the severe weather with the combination of radar. Since the limitation of data, we choose the lightning data from 1989 and 1990 only for preliminary analysis.

In addition, the thunderstorm day and thunder density are two important meteorological parameters for weather observation and lightning protection in electric power, construction and space flight. Qie et al. (1989) found that the thunderstorm day got from lightning data of LLS is in good agreement with that from meteorological observatory. This paper tries to give the thunderstorm day, thunder density and thunderstorm hour in different regions covered by LLS by using lightning data of LLS. It is expected that more scientific, more detailed and more objective data can be provided.

II. DATA COLLECTION AND CHARACTERISTICS

The lightning location data were obtained from a network in Beijing consisting of 3 DFs and one PA. Being 35 km apart from each other, each DF is pre–set to run on medium–range gain with a specified detection range of less than 180 km. The information from DFs including lightning occurring time, direction, strength and return strok number is transmitted to PA where the location of each flash is computed by triangulation method in real time. The LLS has been well equipped with a graphic display system which indicates the lightning location in past or real time and discriminates the lightnings occurring in different time with different colors. The system can be used to track and monitor the presence and motion of the storm in combination with Doppler radar and satellite.

This system works on a low and very low frequency bandwidth with the wavelength from 300 m to 300 km. The electromagnetic wave between these frequencies propagates along the earth's surface almost without attenuation and distortion within hundreds of kilometer. The reflection caused by mountain and building can be ignored. The diffraction along mountain is the main propagation mode. So it is believed that lightning radiation field propagates along the earth's surface and mountains. LLS can eliminates the shortage of other detection tools such as radar which is affected by topography.

The positions of flash are obtained by using the simultaneous direction vectors of 3 DFs. The system has high direction accuracy due to responding only to the peak radiation field of cloud–to–ground flash when the top of flash channel is still about 100 m above the ground and the channel is basically perpendicular to the ground. However the site error, arisen from the displacement of antennas, near buildings and metallic objects, may be very high, sometimes as high as 10 degrees. So the lightning location data are corrected by using a parametrization method (Chen et al., 1991).

III. THE APPLICATION OF LIGHTNING DATA

Convective storm is often accompanied with severe lightning activity. There is a strong coupling and feedback between dynamic and electric processes in storm. It is possible to discuss the increasing process of dynamics and to forecast some characteristics in storm by using lightning data. Based on the observation experiences and data analyses during these two years, some applicable aspects of lightning data are summarised as follows.

1. *Determination of Thunderstorm Day, Thunder Density and Thunderstorm Hour in Different Regions*

The lightning location data detected by the LLS may be used to calculate the regional distribution of thunderstorm day (T_d), thunder density (N_g) and thunderstorm hour (T_h) in the area covered by the LLS. After many year's observation, it may have more reliable data than those obtained by traditional method.

The traditional thunderstorm day is defined as a day during which as long as the thunder is heard at the station. Because of sound wave attenuation during propagation and resolution limitation of human's ear, the farest range of thunder heard by ear is about 25 km, corresponding to an area of 1900 km^2. To compare with this area, the lightning data were referenced to the grid blocks that are approximately 44×44 km^2. We have defined the thunderstorm day as a day during which as long as lightning appears on the grid. The total grid number is 49 within an area of about 100 000 km^2.

The detecting area includes the northern North China Plain and southeast Mongolian Plateau. In west and north parts are rolling hills with an average elevation of 1000—1500 m above sea level. In the southeast, the hills become lower and lower gradually in the direction from northwest to southeast and then go into a great plain. About 60% out of the detecting area is the mountainous region. The mountainous region in west belongs to Taihang Mountain chain which includes a series of approximately parallel hills in the direction from northeast to southwest. The mountains in north is the Jundu Mountain which belongs to Yanshan Mountain chain. There are many rivers in the detecting area, such as Yongding River, Chaobai River and Daqing River which flow to the Bohai Sea.

Table 1. The Distribution of T_d, N_g and T_h in Grids A1—G7

	1	2	3	4	5	6	7
A	3 (T_d) 0.001 (N_g) 22 (T_h)	14 0.005 33	14 0.010 43	10 0.008 28	8 0.008 26	13 0.016 25	15 0.013 27
B	8 0.002 23	18 0.017 48	27 0.021 28	14 0.010 48	11 0.008 47	14 0.019 42	13 0.011 31
C	19 0.006 23	22 0.023 48	30 0.019 48	20 0.017 48	15 0.022 41	20 0.013 42	19 0.009 31
D	10 0.005 22	13 0.014 29	18 0.011 43	31 0.022 105	31 0.036 55	24 0.025 50	15 0.010 42
E	25 0.024 45	23 0.013 26	21 0.010 41	21 0.018 41	22 0.024 93	16 0.012 18	10 0.004 19
F	15 0.009 15	20 0.009 26	15 0.012 41	11 0.008 101	13 0.004 93	16 0.010 18	10 0.004 19
G	15 0.009 28	20 0.009 41	15 0.013 37	11 0.008 79	13 0.004 50	16 0.010 47	10 0.004 24

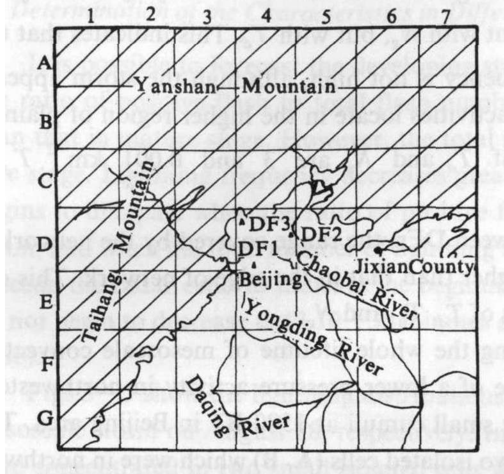

Fig. 1. Region division and distribution of DF stations, the width of each grid is 44 km.

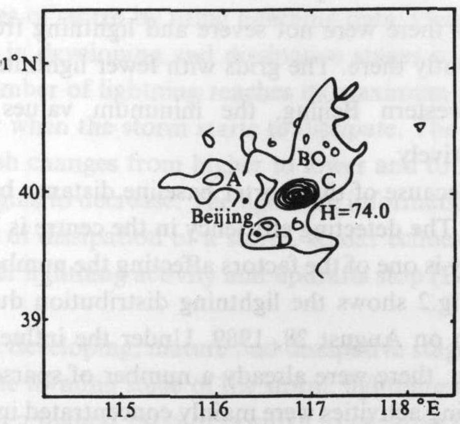

Fig. 2. The lightning distribution during whole lifetime of the storm on August 28. The isopleth is given based on the lightning number in the grid of 10 × 10 km^2. The total number of grids is 60 × 60 corresponding to an area of 600 × 600 km^2. The outmost contour represents 1 lightning per grid, and the interval of contours is 10.

The complicated topography has strong influence on local circulation during summer. In the higher mountainous region, air is heated earlier and the cloud forms first because of the influence of global atmospheric circulation. The area has a typical continental monsoon climate and has a lot of thunderstorms in summer.

Table 1 is the distribution of thunder density, thunderstorm day and thunderstorm hour around Beijing from June 30 to September 14, 1989. The numbers at the low–right, up–left and up–right corners are thunderstorm hour T_h, thunderstorm day T_d and thunder density N_g (km^{-2} T_d^{-1}), respectively. The thunder density refers to the average lightning number occurring within a unit area during a thunderstorm day.

Obviously, the storm activity varies with different regions. The shape formed by grids with more lightning activities is almost the same as the boundary of mountains, i.e. along the east side of Taihang Mountain from south to north, then along the south side of Yanshan Mountain eastward. This region is hilly zone connecting plain with mountain. Because of the sufficient sunshine and the terrain elevation, the convective activity is easier to form, and the thunderstorm activity occurs more frequently there. The peak thunderstorm day and thunder density occurring in the region between Jixian County and Beijing (Grid D5). T_d on D5 is 31, N_g is 0.036 km^{-2} T_d^{-1} and T_h is 55. T_d and N_g on D5 reach their maximum value, but T_h there is much lower than its maximum value, 105. This suggests that the lightning frequency is very high as long as the storm is developing. It may represent that severe convective activities often occur in this area. The maximum of T_h, 105, is in the grid which covers the Beijing with T_d 31, N_g 0.022 km^{-2} T_d^{-1}. T_h is not in good agreement with N_g, but with T_d. This indicates that the storms there were not severe and lightning frequency is not high, although the storm appears frequently there. The grids with fewer lightning activities locate in the higher region of plain in northwestern Beijing, the minimum values of T_d and N_g are 3 and 0.001 km^{-2} T_d^{-1}, respectively.

Because of the shorter baseline distance between DFs, the range covered by the network is small. The detecting efficiency in the centre is higher than that in the edge of network. This obviously is one of the factors affecting the numbers of T_d, T_h and N_g.

Fig.2 shows the lightning distribution during the whole lifetime of mesoscale convective system on August 28, 1989. Under the influence of a lower pressure activity in northwestern Beijing, there were already a number of sparsely small cumuli at 1500 BT in Beijing area. The lightning activities were mainly concentrated in two isolated cells (A, B) which were in northwest and northeast respectively. Cell A was near the Yongding River. The maximum reflectivity at 1800 BT was 30 dBz. After that these two cells closed up gradually and moved southward. At 2000 BT, several small cells merged into a bigger, severer multicell storm gradually, and became strengthened and matured in the region between Beijing and Jixian County south of Yanshan Mountain chain and stayed there for a long time (C in Fig.2). This region is not only the boundary area of the plain and Yanshan Mountain but also within the Chaobai River area. At 2336 BT, PPI echoes indicated that the maximum echo area appeared and then became smaller and smaller. It moved southward slowly when it approached to dissipative stage. The grid with the maximum lightning number 74 located at the region 70 km east of and 10 km north of Beijing. This kind of storm is very typical during our observation period from 1989 to 1990. In the most cases, the severe mesoscale convective storm formed in the boundary area of Yanshan Mountain chain and Taihang Mountain chain or in the sunny side of the mountains, and went along the ridge of mountains while its development was accelerated and intensified by the mountains. This is why the highest thunder density appears on the south side of the Yanshan Mountain.

Above lightning distribution indicates that the boundary area of mountain and plain (such as D4, D5, D6, C4, C5) is the area where convective activity is most severe and stable. Affected by topography and sunshine, lightning activity varies greatly with different areas. Different topography and sunshine conditions cause various convective activities with different intensities. The thunderstorm day and thunder density also vary stably with it. Listed in Table 1 are the thunderstorm day results obtained from a number of lightning data observed during the summer of 1989. These results are more detailed and accurate than the results from the traditional thunderstorm day observation method. Because of the shortage of observatory in the mountainous region and the limitation of human ear, there are limitation, subjectivity and inconvenience in obtaining the accurate thunderstorm day distribution in detail. However, the distribution of T_d, N_g and T_h in any region within the detecting area can be provided in detail by using the LLS data, especially in the area without observatory. LLS is a perfect detecting tool for it is not affected by topography and is not limited by the field of vision and time delay. The LLS data can also be used to monitor the storm activity and to provide meteorological data in more detail.

2. *Determination of the Characteristics in Different Developing Stages of Storms*

It is possible to forecast the developing stages of storm by using lightning data. Generally, the ratio of positive flash to total flash number in developing and dissipative stages is higher than that in mature stage. However, the total number of lightning reaches its maximum in mature stage. Lightning frequency decreases greatly when the storm starts to dissipate. The storm begins to dissipate when the ratio of positive flash changes from higher to lower and to higher again, and when the total number of lightning begins to decrease. The lightning information can precede the radar echo to indicate the beginning of dissipation of a storm. Radar echoes often do not begin to decrease until 10—30 minutes after lightning activity and updrafts stop (Edman, 1986).

Figs.3—5 show the lightning distributions in developing, mature and dissipative stages in a mesoscale storm on August 28, respectively. In the forming stage of the storm, lightning flashes were concentrated in two small isolated cells with a highest ratio of positive to negative flashes of 25.3%, while the number of negative flash was 413. The highest positive flash ratio was probably due to the positive charges at the lower part of storms. In the mature stage, lightning flashes were more concentrated and the two original cells merged into one bigger cell which moved southward with higher lightning frequency. At that time the maximum lightning number per grid was 72, the ratio of positive to negative flashes was 2.5% with the total negative flash number 1136. Total lightning number was 98 with a ratio of positive to negative flashes 11.4% in the dissipative stage.

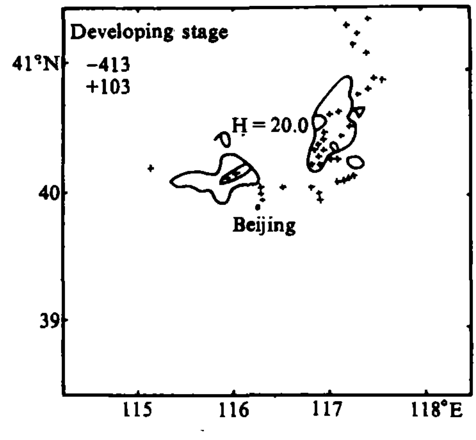

Fig. 3. The lightning distribution in the developing stage. Contours are drawn based on the number of negative flashes on grid of 10 × 10 km^2. The outer contour represents 1 negative flash per grid. Interval between contours is 10. "+" represents the location of positive flash.

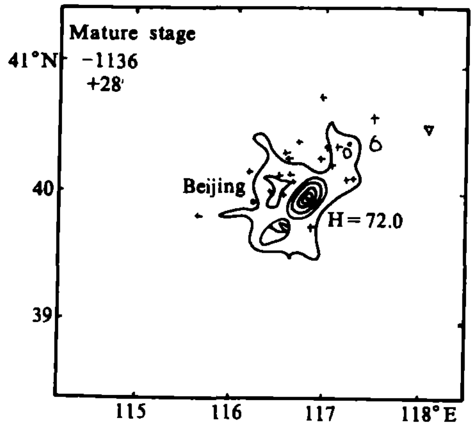

Fig. 4. As in Fig.3, but for mature stage.

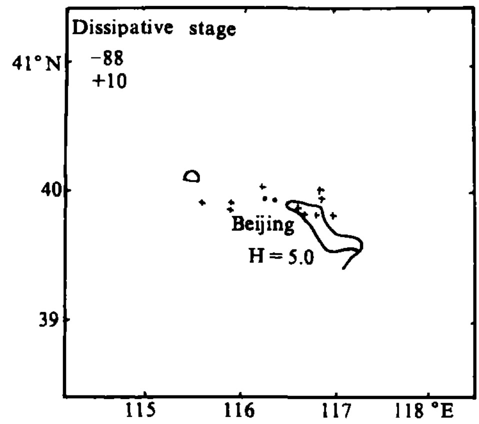

Fig. 5. As in Fig.3, but for dissipative stage.

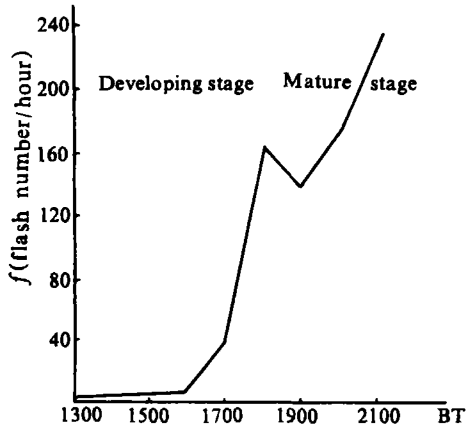

Fig. 6. The variation of lightning frequency in early stage of storm.

The ratio of positive to negative flashes varies from higher to lower and to higher again. Total lightning number is higher in mature stage than that in forming and dissipative stages. From this case analysis, it is concluded that different developing stages may be determined roughly by the positive lightning ratio and lightning frequency. In fact, several samples of severe, large scale convective storm, such as storms on July 13, 1989, August 7 and 11, 1990, support this conclusion.

In addition, the negative flashes are more concentrated than positive flashes, especially in developing and dissipative stages. This has been discussed by Yan et al. and Ge et al. (1992) in detail. The emphasis in this paper will be put on the storm forecasting.

3. *The Nowcasting of Storm*

(1) *Determination of the convective region and its developing possibility*

The processes of charge separation, accumulation and lightning discharge are closely related to the convective activity. However the updraft often appears first during the lifetime of a storm. It may be possible to infer the convective region, its location and the possibility of further developing. In the region where can not be detected by radar or where no radar is installed, lightning data may be used to forecast the existence of a storm in combination with satellite data. Particularly for the storm with lower cloud top or impeded by heavy rain or thick cloud, lightning data have more advantages.

Fig.6 shows the time sequence variation of lightning frequency (the lightning number per hour within 30 minutes before and 30minutes after the moment) during the earlier stage of mesoscale convective storm on July 13, 1989.

On that day, the first lightning occurred at about 1243 BT, so the convective activity appeared before that moment, but still had no radar echoes corresponding to it. The lightning frequency went up evidently with the developing of storm although there were small fluctuations on it. This indicates that the storm was becoming severe gradually. When the storm had been in vigorous period of mature stage, lightning frequency changed from 3 h^{-1} at 1300 BT to 233 h^{-1} at 2100 BT. Based on the above analysis it is possible for us to forecast the further development of a storm by using the time sequence variation of lightning frequency.

(2) *Regional thunderstorm forecasting*

Referring to the lightning data and radar echoes with intensity greater than 30 dBz occurring in the severe storm on July 13 and that on August 28, 1989, we find that there are not always active radar echoes (greater than 30 dBz) in the grids with lightning (lightning occurring within 10 minutes with the moment being mid–point). Moreover, the grid with the maximum lightning number may be in the region without active echoes. Sometimes there was a horizontal distance of about several ten kilometers between them. But, there will be a centre of active echoes in the grids with the maximum lightning number after 30 minutes to an hour. The sample analysis suggests that the locations of intensive radar echoes may be forecasted by using the grid lightning data obtained 30 minutes to an hour before. An example of regional nowcasting for the storm on August 28 is as follows.

Lightning data in the present study are referred to those in many 10×10 km^2 grids. Each grid is represented by A—J in column, 1—10 in row, respectively. Beijing is in F1, so the region discussed is bounded by 55 km northward and 45 km southward to Beijing, and from Beijing to 100 km eastward to Beijing.

At 2000 BT, August 28, most of lightning entered the region. Table 2 shows the lightning distribution from 2000 BT (including 2000, 2010, 2020 and 2030) to 2300 BT (including 2300, 2310, 2320 and 2330), with the time interval of 1 hour. The number in each grid represents the number of lightning occurring 5 minutes before the moment.

At 2000 BT, C5 had the maximum lightning number, 7. In B4, D4 and B5 there were some lightning flashes also. From moving direction of lightning before 2000 BT, it was inferred that the intensive echo was in the north of the region discussed and was moving toward this region. The centre of active radar echoes would be close to C5 one hour later. Table 3 shows the horizontal distribution of active echoes at 2000, 2100, 2200 and 2300 BT. At 2000 BT, most of the grids with lightning including C5 had no active echoes. However, it is found that C5 was filled by active echoes at 2100 BT and most of grids with lightning at 2000 BT were also covered by active echoes at 2100 BT. The lightning on E9 and E10 also indicated that there would be severe convective activities. At 2010 BT, the center of lightning activity began to move southward. The maximum lightning number moved into D5. The distribution of lightning at 2010 BT was in good agreement with that of echoes at 2100 BT. At 2020 and 2030 BT, the grids with lightning began to move toward southwest. Grid E8 got maximum lightning number at 2030 BT. It is noted that the cell on E8 would be the centre of active echoes one hour after.

At 2100 BT, E9 was the centre of lightning, it is expected that E9 would be the centre of active radar echo at 2200 BT. Another lightning peak on J2 was generated by another isolated cell. It would be the centre of another cell an hour later. E9 was the centre of active echoes at

2200 BT, and there were active echoes at 2100 BT also. J2 had active echoes at 2200 BT and no active echoes at 2100 BT. So the lightning on J2 at 2100 BT forecasted the development of new cells an hour later. The grids with more lightning flashes at 2100 BT were in accordance with the distribution of echoes at 2200 BT. Between 2110 BT and 2130 BT, the lightning flashes were basically in accordance with the active echoes at 2200 BT. However, the storm continued to move southward in reference to the lightning distribution. This was proved by the distribution of echoes at 2300 BT.

At 2200 BT, lightning flashes were distributed on many grids. The two cells centered on E9 and J2 an hour ago were closed together gradually. Lightning in I4 forecasted the centre of active centre at 2300 BT. Another subpeak of lightning number in E8 did not forecast the active echoes. In addition, the merger of two cells indicated by lightning data at 2200 BT was verified

Table 2. The Distribution of Lightning Number during 10 Minutes

a

2000 BT

	1	2	3	4	5	6	7	8	9	10
A					1					
B				3	2			1		
C			1	1	7					
D				3					1	1
E			1				1		3	3
F		2	2				1			
G										
H										
I										
J										

2010 BT

	1	2	3	4	5	6	7	8	9	10
A										
B			1	1	2	1				
C			1	1	2	1				
D	1			2	7					
E		1	2	4				1	1	1
F			4		1					
G										
H										
I										
J										

2020 BT

	1	2	3	4	5	6	7	8	9	10
A							1			
B						1				
C				2	1	2			1	
D	1	1		3						
E		1	1					2	2	1
F	5	1	5							
G	3									
H										
I										
J										

2030 BT

	1	2	3	4	5	6	7	8	9	10
A								2		
B					1	2	5			
C			1			3				
D				3					2	
E							4	7	1	1
F	6	2	1	1						
G	1									
H										
I										
J										

b

2100 BT

	1	2	3	4	5	6	7	8	9	10
A										
B							1	1		
C										
D								1		6
E			1		1	2	1	6	7	1
F	1									
G										
H										
I			2							
J		6	5							

2110 BT

	1	2	3	4	5	6	7	8	9	10
A										
B							1			
C				1						
D								4	4	1
E					1		9	7	5	1
F				1						
G										
H										
I			8							
J		2	3							

2120 BT

	1	2	3	4	5	6	7	8	9	10
A										
B					1					
C								1		
D					1	1		5	3	2
E				1	3	2	8	8	5	
F				1	1	2				
G										
H										
I										
J			3							

2130 BT

	1	2	3	4	5	6	7	8	9	10
A				1						
B								1		
C										
D								1	3	1
E				1	1	1	4	8	3	
F				1		1	5		1	
G							2			1
H										
I			1	1						
J										

c

2200 BT

	1	2	3	4	5	6	7	8	9	10
A										
B										
C									1	
D										
E				1			3	7	1	1
F							2		1	
G				1			2			
H				2			1	2	1	
I			3	8	4			1	3	
J		1	2	1	1	1				

2210 BT

	1	2	3	4	5	6	7	8	9	10
A										
B										
C										
D										
E						1			1	2
F					2		2	2	2	
G								1		
H				1	1		1	1		1
I				4	6	5				1
J					5	7	1	1	1	

2220 BT

	1	2	3	4	5	6	7	8	9	10
A										
B										
C										
D								2		
E								2		
F				2						
G						1				
H										
I	2		3	6	1			1		
J		1		1	1			1	1	

2230 BT

	1	2	3	4	5	6	7	8	9	10
A										
B										
C										
D										1
E										1
F								1		
G			1							
H							2			
I				1	2			1	1	
J		1			7	1				

d

2300 BT

	1	2	3	4	5	6	7	8	9	10
A										
B										
C										
D										
E										
F				2						
G										
H										
I						1		1		
J				1				2	2	

2310 BT

	1	2	3	4	5	6	7	8	9	10
A										
B										1
C		1								
D										
E										
F							1		2	
G						1				1
H										
I										
J										

2320 BT

	1	2	3	4	5	6	7	8	9	10
A										
B										
C										
D										1
E										
F								1		
G	1				1					
H										
I								1	1	
J										

2330 BT

	1	2	3	4	5	6	7	8	9	10
A										
B										
C										
D								1		
E				1						
F										
G										
H										
I								1	1	
J				1						

at 2300 BT. The lightning distribution at 2210 BT was much better than that at 2200 BT for forecasting the active echoes at 2300 BT. At 2220 and 2230 BT, the centre of lightning flashes moved outside the region discussed although the grid with maximum lightning number did not change. The centre of lightning flashes at 2220 and 2230 BT were in good agreement with the active echo at 2300 BT in the region discussed.

At 2300 BT, most of grids with lightning had active echoes, lightning data were in good agreement with radar echoes. However the centre of lightning moved outside the region from south side, and the storm expanded still southward.

Table 3. The Distribution of Active Echoes with Its Intensity Greater than 30 dBz

	1	2	3	4	5	6	7	8	9	10	1	2	3	4	5	6	7	8	9	10	
A	+				+								+	+	+						A
B													+	+	+						B
C													+	+	+	+					C
D												+	+	+					+		D
E												+	+						+	+	E
F																				+	F
G																					G
H																					H
I																					I
J																					J
2000 BT											2100 BT										
A							+	+	+												A
B								+	+	+											B
C								+	+	+											C
D							+	+	+	+											D
E							+	+	+	+										+	E
F								+	+									+	+	+	F
G		+		+									+	+					+		G
H		+										+	+	+				+	+	+	H
I	+	+									+	+	+	+	+			+	+	+	I
J	+	+									+	+	+	+	+	+	+	+	+	+	J
2200 BT											2300 BT										

It is noted that the distribution of active echoes was not in good agreement with the distribution of ground lightning at the same time, when the cell was in the vigorous period and more precipitation particles existed in storm, but in good agreement with that at the previous moment. The reason for this perhaps is that tripole charge structure in the cloud had been well developed during this period and most of lightning flashes at this time were intracloud discharges although the lightning frequency was higher. The positive charges at the bottom of cloud shield the discharges between negative charges at the middle part of cloud and the ground partially. Most of charges are released by intracloud discharges (Wang et al., 1990). However in the edge of intensive echoes, the charges are easier to be discharged to the ground. In the active echo region where the storm has well developed, there are fewer ground lightning flashes while there are many in the edge of the region. As to the echoes in C4 at 2100 and in D8 at 2200 BT,

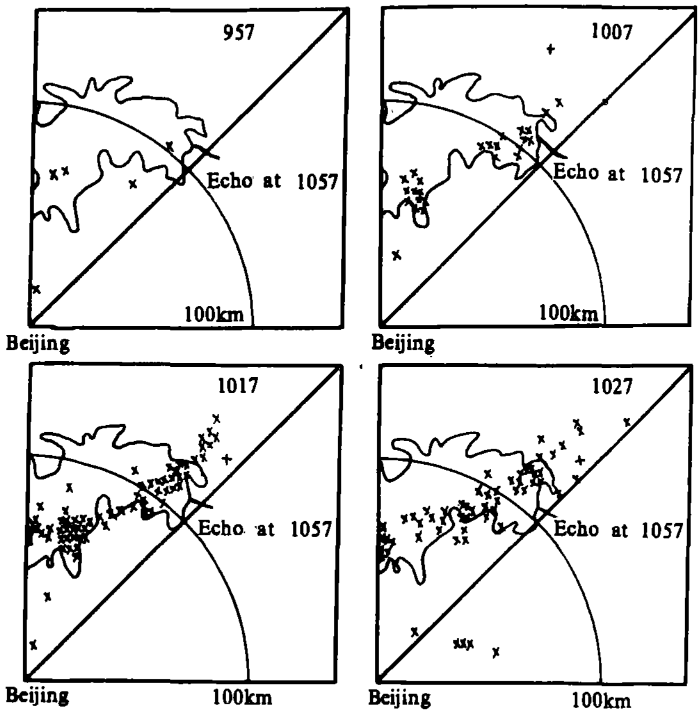

Fig. 7. The comparison of echoes at 1057 BT August 7, 1990 and the lightning locations 30 minutes to an hour before. × indicates the location of lightning.

on August 28, the distribution of lightning at the same moment was not in good agreement with the corresponding active echo. The echoes of storm in these grids were weak and they indicated that the storm there had not well developed. But there were more ground flashes there and the region was covered with active echoes later. So, the ground lightning at previous moment may be used to forecast the development of active echoes, although the lightning distribution may be not in accordance with severe echoes at the same moment.

To illustrate further this phenomenon, Fig.7 shows another comparison of radar echo at 1057 BT with lightning distribution at 30 minutes to an hour before. There were no active echoes within the area in consideration at 0957 BT. It could not be determined whether the echo at 1057 BT was the movement of echoes an hour before or a local new–born cell in the shortage of the continuing echoes. It might be a new–born cell being developing stage by referencing the echoes at 1057 BT. Although there were no active echoes an hour before, lightning at that time had indicated that the active echoes would occur there later. 10 minutes later, there were more lightning flashes in the region and this was a very good indicator of the intense echoes appearing there later at 1057 BT. Lightning at 1027 BT also well indicated the position of active echoes at 1057 BT. In addition, the echoes at 0957 and 1152 BT were also well indicated by the corresponding distribution of lightning occurring 30 minutes to an hour before.

Although the different storm processes and different developing situations cause different charge distributions, and the lightning indication of active echoes appears in different time, lightning may be used to forecast the developing of the convective activity in most of the mesoscale storm as an indicator of active echoes. During the developing and initial mature stages of the mesoscale storm on August 7, it was found that the radar echoes may be indicated by lightning occurring 30 minutes to an hour before from several echoes. In fact, lightning data can indicate the convection earlier. One of the reasons is that the continuing observation of LLS can detect lightning in real time, while the reports of radar, satellite and real situation on ground are limited by time. Another reason is convective mechanism itself. Lightning is the product of charge separation, and it occurs when updrafts cause charge separation. However it needs a long time for the precipitation particles to grow to the size and height which can be detected by radar. In general, lightning may be used to regional forecasting and it can be an hour to 30 minutes earlier than radar for forecasting the approaching of storm.

IV. RESULTS AND DISCUSSION

Cloud–to–ground lightning represents the severe convection, LLS can provide the lightning location information in real time, so the ground lightning data may be used to diagnose and determine the spacial and temporal variation of large–scale storm. Case analysis also suggested the application potentiality of lightning data in nowcasting.

Because of uncontinuous observation of radar and the longer observation interval, it is impossible to track the storm continuously, thus forecasting the intense radar echoes' center by using lightning data occurring 30 minutes to an hour before is a preliminary study. Although the comprehensive indicator can not be found for forecasting the storm characteristics by using lightning data for the limitation of data, this preliminary study gives the concept and possibility of preliminary forecasting by using lightning data. It is expected to further study in combination of satellite, surface report and wind field.

REFERENCES

Chen Mingli, Liu Xinsheng, Guo Changming and Ge Zhengmo (1991), A parametric method of site error estimation of lightning location system, *Acta Meteorologica Sinica*, **5:** 370—380.

Edman, D. A. (1986), Operational use of lightning location on an interactive system, *Proc. 11th Conf. on Weather Forecasting and Analysis*, Amer. Meteor. Soc., pp.165—170.

Fisher, B. and Krider, E. P. (1982), "On–line" lightning maps lead crews to "trouble", *Electra World*, **196:** 11–114.

Ge Zhengmo, Yan Muhong, Guo Changming and Zhang Guangshu (1992), Analysis of cloud–to–ground lightning characteristics in mesoscale storm in Beijing area, *Acta Meteorologica Sinica*, **6:** 491—500.

Jan Lewis (1989), Real time lightning data and its application in forecasting convective activity, *12th Conference on Weather Analysis and Forecasting*, Oct., pp.97—102.

Johnson, R. L., Janota, D. E. and Hay, J. E. (1982), An operational comparison of lightning warning system, *J. Appl. Meteor.*, **21:** 703—707.

Krider, E. P., Noggle, R. C., Pifer, A. E. and Vance, P. I. (1980), Lightning direction finding systems for forest fire detection, *Bull. Amer. Meteor. Soc.*, **61:** 980—986.

Qie Xiushu, Guo Changming and Zhang Guangshu (1989), The site error and application of direction finder for ground flash, *Plateau Meteorology*, **8:** 70—74 (in Chinese).

Rasch, G. E. and Mathewson, M. (1984), Collection and use of lightning strike data in the western U.S. during summer 1983, NOAA Tech. Memo. NWS. WR–184, 36.

Wang Daohong, Liu Xinsheng and Wang Caiwang (1990), A preliminary analysis of the characteristics of ground discharges in the thunderstorms near Zhongchuan, Gansu Province, *Plateau Meteorology*, **9**: 405—410 (in Chinese).

Yan Muhong, Guo Changming, Qie Xiushu, Ge Zhengmo and Zhang Guangshu (1992), Observation and model analyses of positive cloud–to–ground lightning in mesoscale convective systems, *Acta Meteorologica Sinica*, **6**: 501—510.